Serious Sailing: Time-Optimal Control of Sailing Drones in Stochastic, Spatiotemporally Varying Wind Fields

Blake Shepherd¹, Ben Haydon², and Chris Vermillion³

Abstract—In contrast to traditional mobile robots, renewably powered mobile robotic systems offer the potential for unlimited range at the expense of highly stochastic mobility. Robotic sailboats, termed sailing drones, represent one such example that has received recent attention. After providing a detailed model and corresponding velocity polar for a candidate customized robotic sailboat, this paper presents a stochastic dynamic programming (SDP) approach for time-optimal control of sailing drones in a stochastic wind resource, which provides a feedback control policy to minimize expected time to a prescribed waypoint. The paper provides a Monte Carlo study of the impact of wind direction volatility on the resulting routes, along with an assessment of robustness to mismatches between actual and assumed volatility.

I. Introduction

Advancements in the robustness and mobility of robotic systems have given rise to new opportunities for collecting data in uncertain environments that were previously unreachable. Several hostile or remote regions have been explored with the use of autonomous robotic systems, including the surfaces of distant planets, deep waters of the ocean, and the Arctic region [1]. Many desired mobile robotic deployments, particularly those involving meteorological and climatological studies, require the characterization of a spatiotemporally varying system over a very large period of time [2], thereby necessitating persistent exploration. This presents a major challenge for traditional robotic systems, which possess relatively predictable mobility but very limited range, particularly for large payloads. This limited range necessitates recharging stations [3], which in remote or hostile environments are inconvenient at best and completely unavailable at worst.

Out of the desire for unlimited range for conducting persistent missions, significant recent research has focused on the design of renewably powered robotic systems. Examples of such systems include solar powered unmanned aircraft for persistent aerial exploration (see [4]), tumbleweed rovers for remote terrestrial or planetary surface exploration (see [5]), and sailing drones (described in [6], [7] and depicted in Fig. 1) for oceanographic surface exploration.

While these systems are not hampered by limited range, the mission planning and control of renewably powered robotic systems is complicated by stochastic mobility. In particular, the achievable velocities of a renewably powered robotic system, and consequently, the set of reachable locations for a given time horizon, are dictated by a spatiotemporally varying, stochastic resource. This gives rise to two significant mission planning and control challenges:

- Persistent mission planning: Strategically selecting target waypoints without knowledge of the waypoint arrival times (since waypoint arrival times will be dictated by the stochastic, spatiotemporally varying resource);
- Control for maximum mobility: Selecting a route that minimizes the time required to reach a waypoint in a stochastic, spatiotemporally varying resource.

In this work, we focus on the second challenge, namely control for maximum mobility, for a sailing drone application. In fact, several studies have examined the problem of maximizing mobility in sailing applications, through both deterministic and stochastic time-optimal control problems. For example, [8] examines optimal path planning in the presence of direction-dependent velocity functions (which is directly applicable to sailing drones, since achievable velocity is dependent on the boat's direction relative to the wind) and in a deterministic environment. In fact, this work shows that in a deterministic environment, the time-optimal solution involves at most one direction change (a "onetack" solution in the case of sailing). Optimizing mobility becomes more complicated in the presence of stochasticity, and a handful of results have examined this problem in the context of sailing. For example, [9] utilizes SDP to minimize time spent on an upwind leg of a sailing race, whereas [10] performs a subtle transformation of the aforementioned problem by maximizing the odds of winning rather than focusing on pure time optimality. This subtle adjustment is also seen through the application of a utility function in place of pure time optimality in [11].





(a) Saildrone [6]

(b) Datamaran Mark 8 [7]

Fig. 1: Commercial Autonomous Sailboats. Image credits: Saildrone (left), Autonomous Marine Systems (right).

¹Blake Shepherd is pursuing a Master's of Science in Mechanical Engineering at North Carolina State University.

²Ben Haydon is pursuing a Doctor of Philosophy in Mechanical Engineering at North Carolina State University.

³Chris Vermillion is an Associate Professor in the Department of Mechanical and Aerospace Engineering at North Carolina State University, Raleigh, NC 27695, USA

In spite of the appreciable amount of prior research in optimal control of sailing vessels, several key gaps in the literature remain:

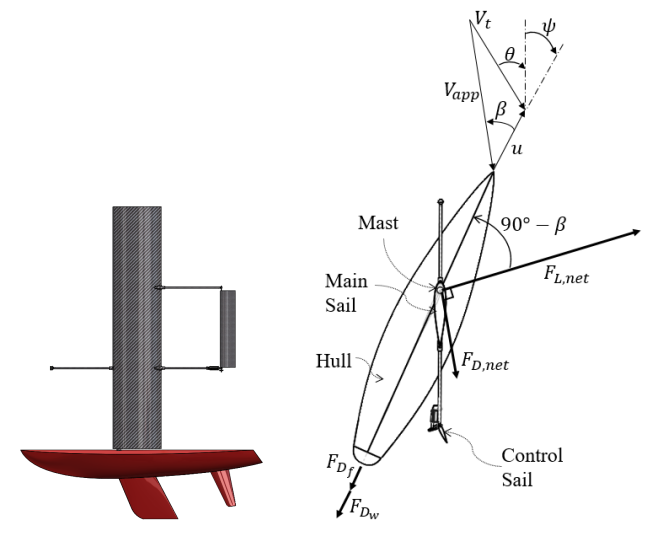
- There does not exist a comprehensive and transparent analysis that evaluates the statistical properties of optimized sailing routes as a function of the statistics that describe the spatiotemporally varying wind resource (as measured through temporal length scales and variance).
- There does not exist an empirical or theoretical result that examines routes in the limits of volatility, which should approach the results of [8] as wind variance approaches zero and/or temporal length scales become sufficiently large.
- There does not exist a comprehensive and transparent assessment of the robustness of SDP-based algorithms to mismatches between the assumed and actual wind volatility statistics.

The present paper addresses the above gaps by providing an analysis of SDP-based time-optimal sailing strategies under a range of wind volatility parameters. In particular, we show how SDP is used to derive a control policy that minimizes expected time to a prescribed waypoint. Focusing on a customized robotic sailboat design based on a Soling 1m hull, we then perform a Monte Carlo study where we simulate the performance of this policy over thousands of randomized wind profiles with specified volatility parameters. We present individual results ("spaghetti plots") and aggregate statistics for the resulting routes. Furthermore, we demonstrate convergence of the SDP result to the deterministic result of [8] when the temporal length scale of the wind exceeds the time scale of the full simulation. Finally, we perform a detailed robustness assessment of the stochastic time-optimal control approach by considering scenarios where the assumed and actual wind volatility differ.

The remainder of the paper is organized as follows. Section II describes the force and moment model for the customized sailing drone under consideration, along with key design parameters. Section III describes the SDP setup for time-optimal control in the spatiotemporally varying wind environment. Section IV summarizes results from a Monte Carlo study of the SDP approach, which provides insight into the behavior of the time-optimal solutions as a function of statistical wind volatility parameters, along with an assessment of robustness.

II. MODELING

In this work, we focus on a customized robotic sailboat design, based on the Soling 1-meter hull, which is depicted in the CAD rendering of Fig. 2 and presently being prototyped within the Control and Optimization for Renewables and Energy Efficiency (CORE) Lab at North Carolina State University. The design incorporates a rigid wingsail and smaller control sail above its hull, which is consistent with existing robotic sailboat designs, guided by principles discussed in [12], and simplifies both modeling and trim. A summary of geometric design parameters is given in Table I.



CAD characterized robotic sailboat design.

rendering of (b) Top view diagram of the autonomous sailboat with aggregate forces and relevant variables

Fig. 2: Autonomous Sailboat CAD Model and Aggregate Force Diagram

A. Basic Dynamic Model

To characterize the dynamics of the proposed design, a high-level model was created using established aerodynamic and hydrodynamic force equations, as detailed further below and introduced in [13] and [14]. Critical geometric variables in this model are shown in Fig. 2, whereas the specific forces acting on the wingsail and trim sail, along with sail-related geometric variables, are shown in Fig. 3. The dynamics that describe the translational motion of the boat are given by:

$$\dot{x} = -u\sin\psi,\tag{1}$$

$$\dot{y} = u\cos\psi, \tag{2}$$

$$\dot{y} = u \cos \psi, \qquad (2)$$

$$\dot{u} = \sum_{i} F_{u,i}, \qquad (3)$$

where $F_{u,i}$ represents the force generated by component i in the boat's longitudinal direction. Based on Fig. 2, Eqn. (3) can be written as:

$$\dot{u} = F_{L,net}\sin(\beta) - F_{D,net}\cos(\beta) - F_{D_f} - F_{D_w}, \quad (4)$$

where β is the apparent wind angle, $F_{L,net}$ and $F_{D,net}$ are the respective net lift and drag forces acting acting on the wingsail, and F_{D_f} and F_{D_w} are hydrodynamic drag forces further described in the ensuing subsections. The apparent wind is defined to be the vector difference of the true wind. V_t , with associated wind angle θ , and the velocity of the boat, u, with associated heading, ψ . Ultimately, this model was used to derive a velocity polar for the intended design, which characterizes the steady-state speed at which the sailboat can travel, as a function of the true wind speed and the heading of the wind relative to the boat.

B. Aerodynamic Forces and Moments

The rigid wingsail assembly (which incorporates a mainsail and separate control sail) rotates about the mast and can

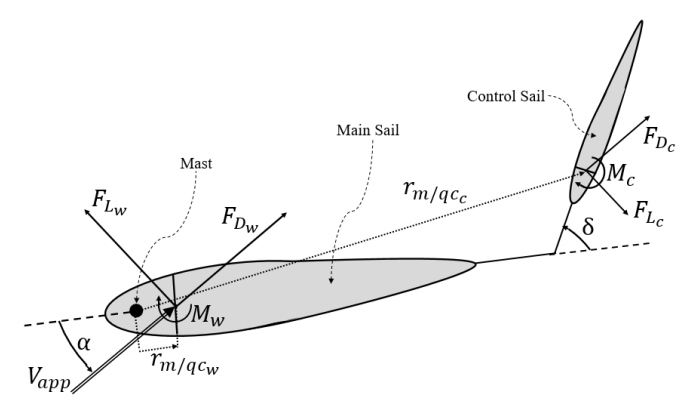


Fig. 3: Free body diagram showing the forces and moments acting on the wingsail assembly.

be represented by the free body diagram shown in Fig. 3. Under steady state conditions, there will be no rotation of the sail about the mast; thus, it must be true that:

$$\sum \vec{M}_{\text{mast}} = 0.$$
 (5)

For any arbitrary mast and control surface pivot locations, which should be ahead of the quarter chord location of each respective airfoil for stability reasons beyond the scope of this paper, equation (5) implies that:

$$0 = \vec{r}_{m/qc_w} \times (\vec{F}_{L_w} + \vec{F}_{D_w}) + \vec{r}_{m/qc_c} \times (\vec{F}_{L_c} + \vec{F}_{D_c})$$

$$- (\vec{M}_w + \vec{M}_c),$$
(6)

where the subscripts w and c denote variables associated with the main wing and control sail, respectively. With this convention, \vec{r}_{m/qc_i} represents a vector from the mast to the the quarter chord of the specified airfoil. The forces due to lift, \vec{F}_{L_i} , and drag, $\vec{F}_{D_{\vec{i}}}$, as well as the resulting moment about quarter chord, \vec{M}_i , can be written in terms of the density of air, ρ , the velocity of the apparent wind, \vec{V}_{app} , and the area of the corresponding surface, S as:

$$\vec{F}_{L_i} = \frac{1}{2} \rho \vec{V}_{app}^2 C_L S,\tag{7}$$

$$\vec{F}_{D_i} = \frac{1}{2} \rho \vec{V}_{app}^2 \left(C_{D,0} + \frac{C_L^2}{AR\pi e} \right) S,$$
 (8)

$$\vec{M}_i = \frac{1}{2}\rho \vec{V}_{app}^2 C_M Sc, \tag{9}$$

where coefficients C_L and C_M are functions of the angle of attack, α , and deflection angle δ for equations associated with the control surface, whereas $C_{D,0}$ represents parasitic drag at the zero-lift angle of attack. The remaining variables are associated with parameters of the wing, where c represents the chord length, AR is the aspect ratio, and e is the Oswald efficiency factor given by the shape of the wing. For the rectangular plan view geometry used for both the mainsail and control sail, AR = s/c, where s is the span and S = sc. Values for these parameters are given in Table I. Both aerodynamic surfaces are characterized by symmetric NACA 0018 airfoils.

Parameter	Value	Description
s_w	1 m	Span of the main sail
s_c	0.316 m	Span of the control sail
c_w	0.2 m	Chord length of the main sail
c_c	$0.063 \ m$	Chord length of the control sail
S_w	$0.2 \ m^2$	Reference area of the main sail
S_c	$0.02 \ m^2$	Reference area of the control sail
AR	5	Aspect ratio of both main and control
		surface surface airfoils
e	0.85	Oswald efficiency factor of each airfoil
d_{sep}	$0.25 \ m$	Separation distance from trailing edge
		of main sail to leading edge of control sail
r_{m/qc_w}	$0.025 \ m$	Distance from mast location to quarter
		chord of the main sail
r_{p/qc_c}	$0.005 \ m$	Distance from the control sail pivot
-,		to the quarter chord of the control sail
LOA	1 m	Length overall of the Soling 1-meter hull
S_{hull}	$0.2 \ m^2$	Wetted surface area of the hull
Draft	$0.254 \ m$	Distance from the bottom of the keel
		to the waterline
L_{wl}	$0.965 \ m$	Length of waterline on hull
Beam	$0.229 \ m$	Width of hull at widest location

TABLE I: Design Parameter Values

C. Hydrodynamic Forces

The hull, as shown in Fig. 2, was modeled based on the Soling 1-meter [15] design, which will be used for future experimental validation of the control strategies developed in this work. Hull hydrodynamic drag forces are computed as:

$$\vec{F}_{D_f} = \frac{1}{2} \rho_w \vec{U}^2 S_{\text{hull}} C_f, \tag{10}$$

$$\vec{F}_{D_w} = \frac{1}{2} \rho_w \vec{U}^2 S_{\text{hull}} C_w, \tag{11}$$

where \vec{F}_{D_f} represents frictional drag and \vec{F}_{D_w} represents wave drag. In the above equations, ρ_w is the density of water, \vec{U} is the speed of the hull relative to the water ($\vec{U}=\vec{u}$ in calm water with no side slip), and $S_{\rm hull}$ is the wetted surface area of the hull. The frictional drag coefficient, C_f , is a function of the Reynolds number using a characteristic length of $0.7L_{wl}$, and L_{wl} is the length of the waterline. The wave drag coefficient, C_w , is a function of the Froude number and can be approximated using the techniques described in [14].

D. Velocity Polar

The velocity polar characterizes the achievable steady-state forward velocity, u_{ss} , as a function of two variables: (i) the true wind speed, V_t , and (ii) the true wind direction relative to the boat, denoted by TWA and given by TWA = $\psi - \theta$. This is computed by solving for the value of u that renders the total longitudinal force acting on the boat, $\sum_i F_{u,i}$, equal to zero under the assumption that the angle of attack α is chosen such that the net force on the sail in the direction of motion is maximized. Contours of attainable velocities are plotted on a polar map, where the radial coordinate represents the attainable velocity (u_{ss}) and the circumferential coordinate represents TWA.

Fig. 4 provides the resulting velocity polar for the chosen design. The polar indicates the obvious feature that no forward motion is possible directly into the wind, and the

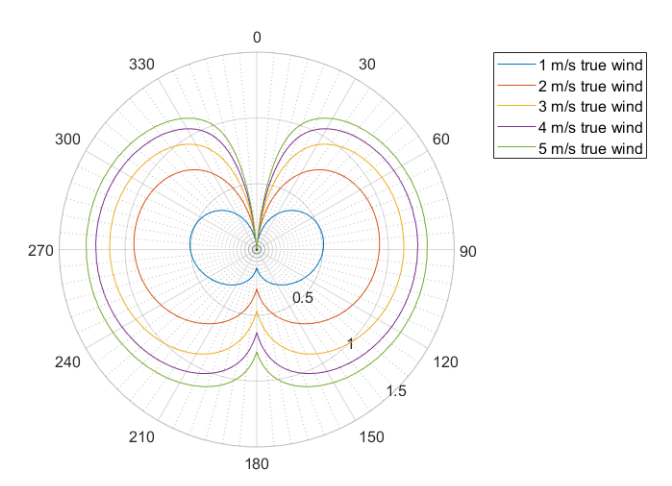


Fig. 4: Boat Velocity Polar

concavity of the velocity polar in this vicinity indicates the degree that the boat should be sailed off the wind to maximize the component of velocity in the intended direction (the "velocity made good"). The velocity polar serves as the basis for developing a time-optimal control law.

III. SDP METHODOLOGY

Our ultimate control objective is to minimize the expected time required to reach a waypoint, given known or estimated statistics regarding the wind environment. For this work, we will focus on an upwind leg of a sailing race, where the mean wind direction vector is directly opposed to the intended direction of travel.

To design this controller, it is first necessary to characterize the environment in which it will operate. To this end, a constant wind speed was assumed, with an associated wind direction that varied according to a Markov model. The transition probabilities associated with the Markov chain follow the following update law:

$$\theta_{i+1} = \theta_i + R(\theta_{\text{prevail}} - \theta_i) + \mathcal{N}(0, \sigma_{tr}^2),$$
 (12)

where θ_i represents the absolute wind direction at step i, θ_{prevail} represents the prevailing wind direction, and R and σ_{tr}^2 are parameters that characterize the volatility of the wind direction. Specifically, R represents the tendency of the wind direction to return towards the prevailing wind direction, and σ_{tr}^2 is the transition variance, or the variance associated with a single transition, or step, in the model. This update law for the Markov transitions can be used to populate a Markov transition matrix where the element in the i^{th} row and j^{th} column can be calculated by:

$$\mathbf{M}_{ij} = \int_{A}^{B} \mathcal{N}(0, \sigma_{tr}^{2}) d\theta$$

$$A = \mu + \theta_{j} - \frac{\delta \theta}{2}$$

$$B = \mu + \theta_{j} + \frac{\delta \theta}{2}$$

$$\mu = \theta_{i} + R(\theta_{\text{prevail}} - \theta_{i})$$
(13)

where \mathbf{M}_{ij} represents the probability of the wind direction transitioning from θ_i to θ_j , and $\delta\theta$ is the step size on the discretization of θ values.

It is more convenient to characterize wind conditions using the overall variance (σ^2) , as well as the time scale (l_t) , which qualitatively represents the amount of time that must pass before a significant change in the wind direction can be observed. Higher values of σ^2 and lower values of l_t correspond to a more volatile wind environment. Subject to proportionality constants k_1 and k_2 , it can be shown that:

$$l_t = \frac{k_1}{R}$$
 and $\sigma^2 = \sigma_{tr}^2 \left(\frac{k_2}{R} + 1\right)$, (14)

Given a probabilistic model of the environmental conditions in which the sailing drones will operate, stochastic dynamic programming (SDP) is a powerful tool for minimizing the *expected* travel time. Specifically, SDP enables the calculation of an expected optimal travel time between a set of waypoints, given a wind model and boat dynamics. The inputs to the SDP solution are the Markov transition matrix, \mathbf{M} , the velocity polar, $u(V_t, \text{TWA})$, and a tacking penalty, λ , along with the course length and width.

In order to formulate the optimal control problem, we discretize the course into a grid of possible x,y positions. The state is fully specified by the boat's x position, current wind angle, θ , and whether the boat is on a port or starboard tack. It is also necessary to store y position as the stage variable. We define our objective function as the expected value of the time to reach a specified terminal waypoint. In order to minimize this time, the decision variable able to be chosen by a controller is the x position at the next y position, which we denote by x'. For each of these states, the stage cost, or cost associated with that particular state transition, is calculated as follows:

$$g(\delta y, x, x', k, \theta) = \frac{\sqrt{\delta y^2 + (x - x')^2}}{u(V_t, \text{TWA})} + c\lambda,$$

$$\text{TWA} = \tan^{-1} \frac{x - x'}{\delta y} - \theta,$$
(15)

where δy is the length of a single stage, x is the current position along the width of the course, x' is the next position along the width of the course, k is a binary variable encoding the current tack, and θ is the current wind direction. The value λ is calibrated to appropriately penalize the amount of time lost due to tacking across a headwind, and c is zero if the current tack matches the previous tack and one otherwise.

Since the first calculated stage costs in a backward recursion are the costs to reach a terminal state from each originating state, they also represent an expected optimal cost to go, denoted $G(x,y,k,\theta)$. After calculating the cost to go from each state that can reach the set of terminal states, the cost to go is then calculated via backward recursion for any state that can reach any of those states as follows:

$$G(x, y, k, \theta) = \min_{x'} [g(\delta y, x, x', k, \theta) + \sum_{j=1}^{n} W_j G(y + \delta y, x', k, \theta_j)],$$

$$(16)$$

where W_j represents the probability based on the Markov model that the wind direction transitions from θ to θ_j , and n is the number of discretized wind angles. In addition to storing the expected optimal cost to go, the result of the above minimization is stored in an optimal decision matrix denoted as $\Pi(x,y,k,\theta)$. This matrix of policies is implemented according to the following control law:

$$x' = \Pi(x, y, k, \theta), \tag{17}$$

and can be used to simulate the performance of the sailing drone when operating in wind conditions that may or may not match the estimated volatility parameters. The number of required function evaluations scales as $\mathcal{O}(n_x^2 n_y n_\theta n_k)$, where n_x , n_y , n_θ , and n_k represent the sizes of each of the corresponding state variables. Because the number of admissible values of the x state is identical to the number of admissible values of the decision variable, the overall computation time varies with the square of that term.

IV. SDP RESULTS

Using to the methodology presented in the previous section, the expected optimal cost to go as well as an optimal decision matrix were calculated over various wind conditions. For each set of wind conditions, the course length was set to 1600 meters, and the boat was restricted to remain within 800 meters of the course centerline. Each course was also set directly against the prevailing wind direction. The true wind speed was set to 2 m/s, and the initial conditions of each simulation were set with the boat on the centerline of the course with a direct headwind.

By simulating 4,000 sets of wind data according to the respective Markov model, Figs. 5, 6, and 7 were created. Each red line represents the path a sailing drone would take under one of the simulated wind conditions, using the precalculated optimal decision matrix. By plotting 10th, 30th, 70th, and 90th percentile bounds (denoted P_x) on these paths, trends within the optimal decision matrix can be visually interpreted and compared under varying levels of wind direction volatility. Two important conclusions can be drawn from these results:

Parameter	Value	Description
V_t	2 m/s	True Wind Speed
$\delta \theta$	5°	Discretization of Wind Direction
θ_{min}	-45°	Minimum Wind Direction
θ_{max}	45°	Maximum Wind Direction
δy	10 m	Stage Length
y_f	1600 m	Course Length
δx	2 m	x Position Discretization
x_{max}	800 m	Maximum Allowable Deviation from Center
		of Course
λ	5 sec	Tacking Penalty

TABLE II: Model Parameter Values

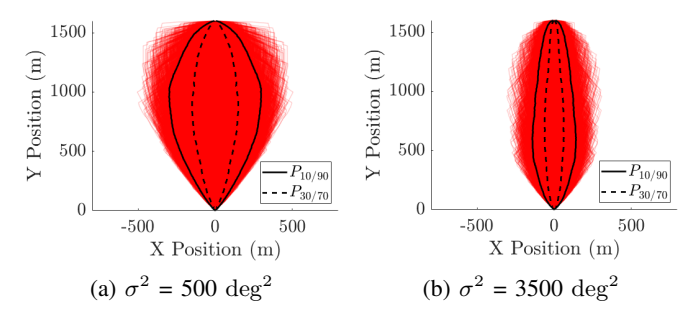


Fig. 5: Simulated boat paths for $l_t = 10$ min. Note that $P_{10/90}$ represents the 10^{th} and 90^{th} percentile bounds on the lateral position along the course, whereas $P_{30/70}$ represents the 30^{th} and 70^{th} percentile bounds.

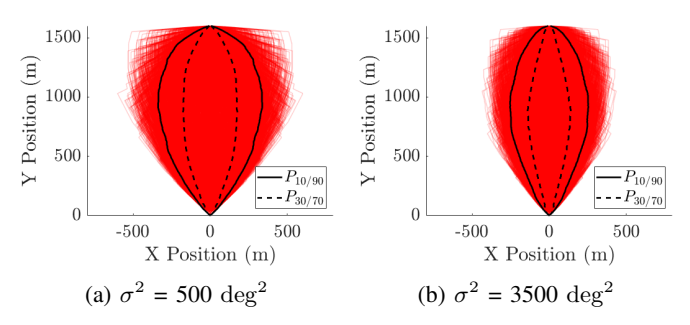


Fig. 6: Simulated boat paths for l_t = 40 min. Note that $P_{10/90}$ represents the 10^{th} and 90^{th} percentile bounds on the lateral position along the course, whereas $P_{30/70}$ represents the 30^{th} and 70^{th} percentile bounds.

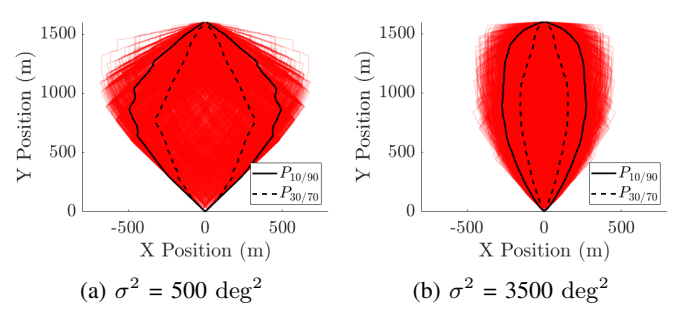
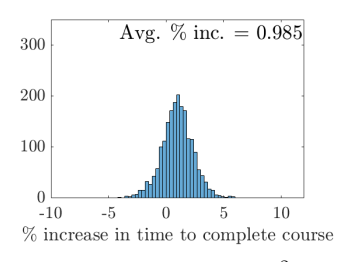
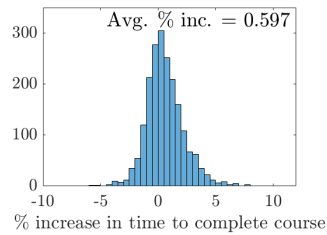


Fig. 7: Simulated boat paths for $l_t = 120$ min. Note that $P_{10/90}$ represents the 10^{th} and 90^{th} percentile bounds on the lateral position along the course, whereas $P_{30/70}$ represents the 30^{th} and 70^{th} percentile bounds.

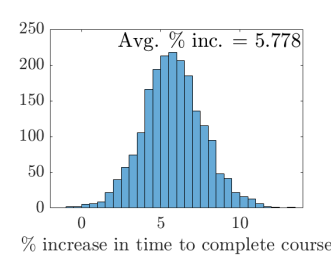
- 1) As volatility gets larger, either through shorter time scales (l_t) or larger variance (σ^2) , optimal routes become tighter. This correlates accurately with sailing rules of thumb, which dictates that it becomes more and more dangerous to explore the extreme left or right side of the course (colloquially termed "banging the corners") as the wind resource becomes more volatile.
- 2) As volatility decreases, particularly when σ^2 is small and l_t exceeds the average total course completion time, the control strategies approach a "one tack" approach, which is proven to be the optimal solution in a deterministic environment in [8].

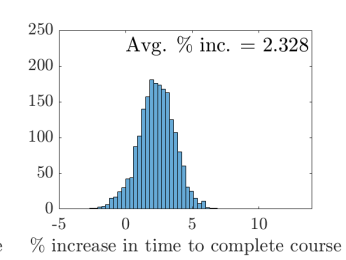




- (a) Underestimating σ^2
- (b) Overestimating σ^2

Fig. 8: Histograms of the percent difference between simulated paths when under or overestimating the overall variance with $l_t = 40 \text{ min}$





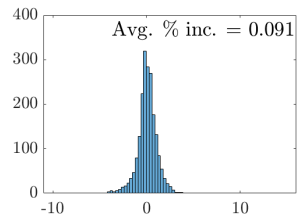
- (a) Overestimating l_t while underestimating σ^2
- (b) Overestimating l_t with accurate σ^2 prediction

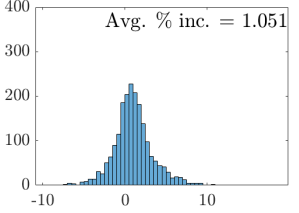
Fig. 9: Histograms of the percent difference between simulated paths when l_t is overestimated

The simulated paths shown in Figs. 5, 6, and 7 are based on the assumption that the estimated parameters, l_t and σ^2 , used to characterize wind volatility, match those experienced by the boat along the course. In reality, the estimated parameters, along with the associated optimal decision lookup table used to run SDP, will not exactly match the actual wind parameters. Figs. 8, 9, and 10 show distributions comparing simulated performance under incorrect wind information to that under correct wind information. The extent to which the differences in the histograms are significant depends on the application (for example, a nearly 6 percent difference in average time is certainly significant in a racing application, whereas it may be less significant in observational missions where the sailing drone is tasked with performing oceanographic assessment). It is also noteworthy that incorrect time scale estimations have a significantly larger impact than incorrect variance estimations. This supports the conclusion that it is more important to understand how quickly the environmental parameters are changing, as compared to how *much* the environmental parameters are changing.

V. CONCLUSIONS AND FUTURE WORK

The paper presented a model, corresponding velocity polar, time-optimal control solution, and detailed simulation results for a robotic sailboat operating in a stochastic, spatiotemporally varying wind field. Results of a Monte Carlo simulation study under various levels of uncertainty confirmed trends in the optimal routes as volatility increases or decreases, demonstrating in particular that the results approach a proven deterministic solution when volatility is extremely low. Finally, a robustness analysis was performed,





- % increase in time to complete course $\,\%$ increase in time to complete course
- (a) Underestimating both l_t and (b) Underestimating l_t while σ^2 overestimating σ^2

Fig. 10: Percent difference between simulated paths under mixed incorrect predictions for l_t and σ^2

which quantified the performance degradation resulting from various levels of mismatch between the estimated and true wind environment. Future work will focus on the extension of the results within this paper to more general waypointto-waypoint paths and the development of heuristic control laws that approximate the results of the SDP optimization while enhancing implementation simplicity and tunability.

REFERENCES

- J. G. Bellingham and K. Rajan, "Robotics in remote and hostile environments," *Science*, vol. 318, no. 5853, pp. 1098–1102, 2007.
 [Online]. Available: https://science.sciencemag.org/content/318/5853/ 1098
- [2] (2019) Navigating the new arctic (NNA). National Science Foundation.[Online]. Available: https://nsf.gov/pubs/2019/nsf19511/nsf19511.pdf
- [3] M. Quann, L. Ojeda, W. Smith, D. Rizzo, M. Castanier, and K. Barton, "An energy-efficient method for multi-robot reconnaissance in an unknown environment," 05 2017, pp. 2279–2284.
- [4] Airbus' solar-powered aircraft just flew for a record 26 days straight. [Online]. Available: https://www.cnbc.com/2018/08/09/airbus-solar-powered-aircraft-just-flew-for-26-days-straight.html
- [5] A. E. Hartl and A. P. Mazzoleni, "Dynamic modeling of a winddriven tumbleweed rover including atmospheric effects," *Journal of Spacecraft and Rockets*, vol. 47, no. 3, pp. 493–502, 2010.
- [6] Saildrone. [Online]. Available: https://www.saildrone.com/team/saildrone
- [7] Autonomous Marine Systems Inc. [Online]. Available: https://www.automarinesys.com/mark8
- [8] I. Dolinskaya, "Optimal path finding in direction, location and time dependent environments," *Naval Research Logistics (NRL)*, vol. 59, 08 2012.
- [9] R. C. Dalang, F. Dumas, S. Sardy, S. Morgenthaler, and J. Vila, "Stochastic optimization of sailing trajectories in an upwind regatta," *Journal of the Operational Research Society*, vol. 66, pp. 807–821, 2015.
- [10] F. Tagliaferri and I. Viola, "A real-time strategy-decision program for sailing yacht races," *Ocean Engineering*, vol. 134, pp. 129 – 139, 2017. [Online]. Available: http://www.sciencedirect.com/science/ article/pii/S002980181730094X
- [11] A. Philpott and A. Mason, "Optimising yacht routes under uncertainty," 01 2001.
- [12] C. Tretow, "Design of a free-rotating wing sail for an autonomous sailboat," Ph.D. dissertation, KTH Royal Institute of Technology, Stockholm, Sweden, 2017. [Online]. Available: https://kth.diva-portal. org/smash/get/diva2:1145351/FULLTEXT01.pdf
- [13] A. Philpott, R. Sullivan, and P. Jackson, "Yacht velocity prediction using mathematical programming," *European Journal of Operational Research*, vol. 67, no. 1, pp. 13 – 24, 1993. [Online]. Available: http://www.sciencedirect.com/science/article/pii/037722179390319I
- [14] J. A. Keuning, "A bare hull resistance prediction method derived from the results of the delft systematic yacht hull series extended to higher speeds," 2008.
- [15] Soling one meter class website. [Online]. Available: https://solingonemetersite.wixsite.com/soling-one-meter